



An experimental study on high-pressure water jets for paraffin scale removal in partially blocked production tubings

Kabir H. Yar'Adua¹ · Idoko J. John¹ · Abubakar J. Abbas¹ · Kazeem A. Lawal² · Aisha Kabir³

Received: 19 July 2020 / Accepted: 19 September 2020
© The Author(s) 2020

Abstract

The common practice of using chemicals and solid-entrained liquids to remove soft scales in production tubings is associated with a high risk of contaminating the environment and eroding pipe internal surfaces. Due to the suspended solids, the current practices are also characterized by high pumping costs and are more problematic to rotating parts of machinery than freshwater. As a cheap and less risky alternative to these corrosive chemicals and liquids, this paper investigates the feasibility of utilizing multiple high-pressure (HP) water jets for the same objective. A total of 54 experimental trials were conducted to study the effects of four factors on the efficiency of scale removal with multiple flat-fan nozzles at an orientation of 25°. The factors investigated are (1) number of nozzles; (2) spray injection pressure; (3) stand-off distance between the spray nozzle and target scale; and (4) condition of the production tubing: ambient and pressurized. Details of the experimental set-up, equipment and procedure are provided. The results of these controlled experiments show a positive correlation between descaling efficiency and spray injection pressure. The same set of experiments reveals a negative correlation between descaling efficiency and nozzle count, as well as between descaling efficiency and spray stand-off. However, for the scale samples and range of parameters investigated in this study, descaling efficiency did not exhibit significant dependency on the chamber conditions, i.e. ambient versus pressurized. The results of this study provide some insights into the feasibility of multiple HP water jets as a cleaner alternative to the use of corrosive chemicals and solid-entrained liquids to remove soft scales in production tubings in oil fields and other applications.

Keywords Flow assurance · Oil field descaling · Paraffin scales · Descaling efficiency · High-pressure water jets · Soft scales

Introduction

The production and transportation of petroleum from sub-surface reservoirs to end-users are accomplished with circular pipes, which include production tubings, pipelines similar process vessels (Mansoori et al. 2017; Nejad and Karimi 2017). However, it is not unusual for these conduits and conveyance systems to suffer flow restrictions resulting from solids depositions, as well as corrosion failures due to internal abrasion by suspended solid particles (Peng and Guo 2017). These solids, which are often major contributors to flow assurance problems, include natural gas hydrates, waxes, asphaltenes, naphthenates, scales and emulsions (Ragunathan et al. 2020; Leporini et al. 2019; Akinyemi et al. 2018; Theyab 2017; Chi et al. 2016; Borden 2014; Lawal et al. 2012, 2011; Lawal 2011).

As posited by Amjad and Koutsoukos (2010), mineral scales that cause flow restriction concerns in the oil and

✉ Idoko J. John
i.j.john@edu.salford.ac.uk

Kabir H. Yar'Adua
K.Y.A.Hassan@edu.salford.ac.uk

Abubakar J. Abbas
A.J.Abbas@salford.ac.uk

Kazeem A. Lawal
Kazeem.lawal@first-epdc.com

Aisha Kabir
kabeeraysha@yahoo.com

¹ University of Salford, Manchester, UK

² FIRST Exploration and Petroleum Development Company Ltd. (FIRST E&P), Lagos, Nigeria

³ Nile University of Nigeria, Abuja, Nigeria

gas industry include calcium carbonate, calcium and barium sulphates, as well as silica scales, iron scales, and calcium phosphate. In addition to these, there are wax scales, which are common in highly paraffinic hydrocarbons. For ease of discrimination from mineral scales which are more challenging to remove, wax scales are regarded as “soft scales”, reflecting their relative ease of removal (Abbas et al. 2015; Abbas 2014).

In broad terms, scales are of organic and inorganic types. While paraffin and asphaltic materials are examples of the former (Braun and Boles 2007), inorganic scales can be further classified into carbonate and sulphate scales (Vazirian et al. 2015). Examples of carbonate scales are CaCO_3 and FeCO_3 , while their sulphate counterparts include BaSO_4 , SrSO_4 and CaSO_4 (Vazirian et al. 2015; Moghadasi et al. 2003a, b).

In general, the point at which these scales are deposited is a function of the nature of the scale and the compositions of the conveying fluid at the time of deposition. In the reservoir, scales block pores and pore throats, thereby causing formation damages with consequent reduction in productivity, injectivity and ultimate recovery, and consequent reduction in project profitability. In pipelines and surface facilities, they cause severe operational problems (Moghadasi et al. 2003a, b).

According to Vazirian et al. (2015), the process of scale deposition involves two major stages, which are deposition and bonding (adhesion). The deposition stage describes the period of nucleation and adhesion to surfaces rough enough and at conditions suitable for the process. On the other hand, the adhesion stage is characterized by the aggregation of existing crystals and consequent scale build-up. Where possible, the adhesion stage includes the clinging of the scale to a suitable surface.

Organic scales are inherent components of petroleum. Typically, they are in solution with the hydrocarbon at conditions that favour their solubility. However, they are precipitated when the oil reaches some saturation conditions triggered by pressure, temperature and/or composition changes. More specifically, the precipitation of organic scales is caused by temperature changes as well as the evolution of gases and lighter components in the cause of producing, treating and transporting crude oil (Sutton 1976). Carbonate and sulphate scales are also liberated from saltwater, which is always present in petroleum reservoirs as initial connate water, or/and water influx from contiguous aquifers as well as water injection. In a nut shell, scales are prone to deposition in reservoir pores, process conduits and facilities due to changing flow conditions and the flow environments.

To forestall the negative impacts of scales on the oil and gas industry, a two-prong approach has been taken to manage this problem. These approaches are the prevention of scale deposition and removal of scale deposits. Common

methods for preventing scale formation include chemical inhibition (Fulford 1975), dilution (Crabtree et al. 1999) and surface coating (Vazirian et al. 2015). The remediation techniques include (1) the use of chemical dissolvers (Elmorsey 2013; Hamdy et al. 2014); (2) spraying with high-pressure (HP) water jets (Abbas et al. 2015; Abbas 2014); (3) rig-less intervention (Guimaraes et al. 2008); and (4) in the worst case, the replacement of production tubing, which is an expensive major rig operation (Guimaraes et al. 2008).

The use of chemical dissolvers is a relatively cheap technique of scale remediation. However, this technique is associated with the risk of contaminating the environment, for example, surface aquifers and other marine habitats. Also, some of the chemical treatment techniques involve the pumping of solids-entrained liquids. In most cases, the entrained solids have high abrasive potential and can erode pipe internal surfaces. Additionally, solids-entrained liquids, owing to the higher viscosity and density of the resulting mixture, are often associated with higher pumping costs. Furthermore, compared to the use of pure water, solids-entrained liquids present more problems to rotating parts of machinery. Still, in terms of health, safety and environmental (HSE) scorecards, there are genuine concerns about the handling and disposal of unutilised chemical dissolvers and effluents at the end of a remediation operation.

Recognizing the limitations of chemical dissolvers, the use of relatively fresh water has been considered as an alternative. In principle, this alternative technique entails spraying HP water jets at deposits on targeted surfaces. Among other attractions, this relatively new technique promises improvements in ease of operations, scale removal efficiency, HSE performance, while still reducing costs. As a contribution to the current body of knowledge on this subject, this paper investigates some relevant design aspects of scale removal by spraying HP water jets.

This laboratory-scale experimental study provides insights into some of the factors that influence the performance of multiple HP water jets when applied to descale a production tubing, partially blocked by paraffin waxes/scales. In addition, the results obtained present a useful basis for quick decision-making in relation to the design, implementation and optimization of HP water jets for remediating scale problems in an oil field.

Method of study

The study involves carefully designed laboratory experiments that can be categorized into three stages: (1) fabrication of soft scale (wax) samples; (2) testing the suitability of the samples, i.e. oil field waxes; and (3) conducting descaling experiments. Figure 1 illustrates the experimental steps and their dependencies.

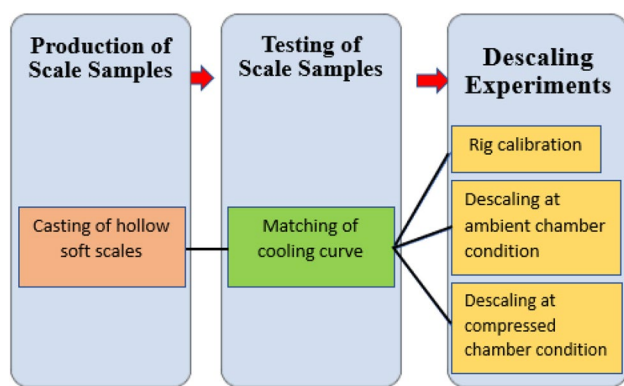


Fig. 1 Workflow for the experiments

To understand the influence of operating pressure on the HP water-jet technique, the descaling experiments were carried out at both ambient and pressurized conditions. These were performed in chambers maintained at ambient and compressed states, respectively.

The soft scale samples used in this study were cast from household candles and tested for their representativeness of actual oil field paraffin waxes. The representativeness testing entailed obtaining the cooling curves for the wax samples and matching same with established cooling curves of typical oil field paraffin waxes, and then comparing the freezing points with the equivalent measurements for corresponding oil field paraffin waxes. Scale samples that passed this test were used in the subsequent descaling experiments while non-representative samples were regretted.

The descaling experiment was conducted in two stages: (1) at ambient chamber condition; and (2) at compressed chamber condition, with the latter simulating field conditions in a typical production tubing. The following sections detail the experimental procedure, including construction and validation of scale samples, calibration of the descaling rig, as well as scale removal at ambient and compressed chamber conditions.

Construction of scale samples

The following is a brief description of the materials and apparatuses as well as other relevant aspects of the construction of the scale samples used.

Materials and apparatuses

All hollow soft scale samples used in this study were cast from household candles and tested for their representativeness of actual oil field paraffin waxes. Apparatuses for this stage of the experiment include safety knife, baking pan, oven, mould, hack saw, kitchen rolls and weighing balance.

The mould, made of thermoplastic materials with high thermal resistant, has two concentric parts. When assembled (Fig. 2), the mould has a height of 15 cm, internal diameter (ID) of 13 cm and outer diameter (OD) of 15 cm. Its melting point is much higher than the temperature of the molten wax.

Casting of hollow soft scales

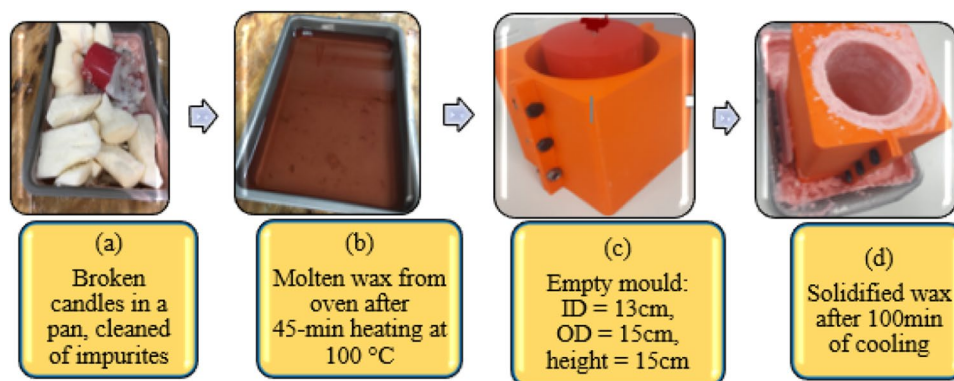
Figure 2 illustrates the four-stage process of scale casting. These stages are (1) candle prepping; (2) candle melting; (3) molten wax pouring and setting; as well as (4) wax cutting and labelling.

Candle prepping entailed breaking the household candles into smaller pieces with the safety knife. Impurities (non-waxy materials), such as candle threads and base plates, were removed from the broken candles. Afterwards, the candle pieces were placed in the baking pan and melted. Candle melting involved placing the pan of clean candles in the oven and heating at 100 °C for 45 min.

After melting, the stage of pouring and setting of molten wax entailed pouring the molten wax carefully into the mould and decanting to remove remaining impurities. The wax was then allowed to cool and set. Average setting time of 100 min was recorded.

At the stage of wax cutting and labelling, each mould was refined to generate two soft hollow scale samples. This

Fig. 2 Fabrication process of hollow soft scales



involves (1) cutting the solid wax sample into two halves, each of length 7 cm, while a 1-cm rough edge was cut off the top half; (2) wiping debris off both waxes with kitchen rolls; and (3) labelling and storing both waxes for subsequent use.

Validation of scale samples

To ensure that the fabricated scale samples were representative of typical oil field paraffin scales, a cooling curve matching test was performed on the molten waxes. The testing materials and apparatus were molten wax and long probe waterproof digital thermometer, respectively.

The validation test involved obtaining the cooling curve for the wax samples and matching it with established cooling curves of typical oil field paraffin waxes. Consistency of the freezing points of the samples versus typical oilfield paraffin waxes was used as the quality indicator. Key steps of the validation test included the following.

1. More than 75% of the thermometer probe was inserted into the molten wax, and the device was switched on.
2. The thermometer was held steady in the above position until temperature readings stabilized.
3. The temperature at that stage was taken and recorded.
4. The above three steps were repeated at two minutes' intervals until the wax solidified.
5. A cooling curve was generated as temperature versus elapsed time. The cooling curve of the wax sample was compared qualitatively (pattern match test) and quantitatively (freezing point test) against published paraffin cooling curves (Hasan et al. 2016; EDGE 2013). Samples that did not satisfy these qualitative and quantitative criteria were rejected.

Descaling (scale removal) experiment

The following sections describe the calibration of the descaling rig for this study, as well as the scale removal experiment under ambient and pressurized descaling chamber conditions.

Calibration of descaling rig

This stage involves the calibration of the entire circulation system of the experimental set-ups shown in Figs. 3 and 4. Specifically, the objectives of this stage of the experiment are to: (1) measure the mass flow rates of water jets through nozzle headers and use these measurements to calibrate the pressure gauges and flow meters; (2) estimate the time-to-fill-up of the descaling chamber for use in setting experimental run time; (3) ensure the integrity of the system and repair any leakages or loose fittings; and (4) to quantify the

pressures at each node, i.e. pump, control board, and descaling chamber.

Descaling at ambient chamber condition

In the present context, ambient condition refers to the absence of any aeration or compression in the tubing chamber. This scenario simulates scale removal from a production tubing at surface conditions, such as a stock-tank environment. In this case, the descaling chamber was maintained at metric standard conditions (MSC) of 101.325 kPa (~1 bar) and 15 °C. Although this scenario is less realistic, the experiment provides a reference for the more realistic scenario of scale removal at compressed chamber condition.

Figure 3 shows the arrangement of materials, instruments and apparatuses employed for descaling experiments under ambient chamber condition. This experiment simulates the use of fresh water to remove paraffin scale deposits in production tubings at MSC when such tubing is not fully plugged by waxes. Freshwater from the mains water supply was sprayed on the scale sample, at the indicated chamber condition, to remove it. "Appendix A" presents an outline of the procedure used to execute this experiment.

Descaling at compressed chamber condition

This scope was designed to simulate the effects of compressive forces generated by the aeration of the descaling chamber on the descaling of production tubing with HP, multiple water jets. In this case, a 2-bar environment was created in the descaling chamber by injecting air and pressurizing it before spraying the scale with HP water. Figure 4 is a schematic of the experimental set-up for this case, while "Appendix B" outlines the laboratory procedure undertaken. An obvious difference between Figs. 3 and 4 is the provision for a compressed (pressurized) chamber and a flowline for air circulation, as well as mechanisms for monitoring the circulated air in the latter case.

Results, analysis and discussion

In line with standard practices, the first step taken in the experimental procedure was to calibrate the rig. The primary objective of this step was to understand the variation of the effective flux of water jet that impinged a scale sample as a function of the nozzle count and jetting pressure. Such understanding would provide an unbiased basis to analyse the results of the various descaling runs. Table 1 provides the results of these initial tests while, to gain better insights, Fig. 5 presents graphical illustrations of the same results.

As would be expected, the mass flux of water injection (i.e. jetting flux) that impinged on a scale sample exhibited a

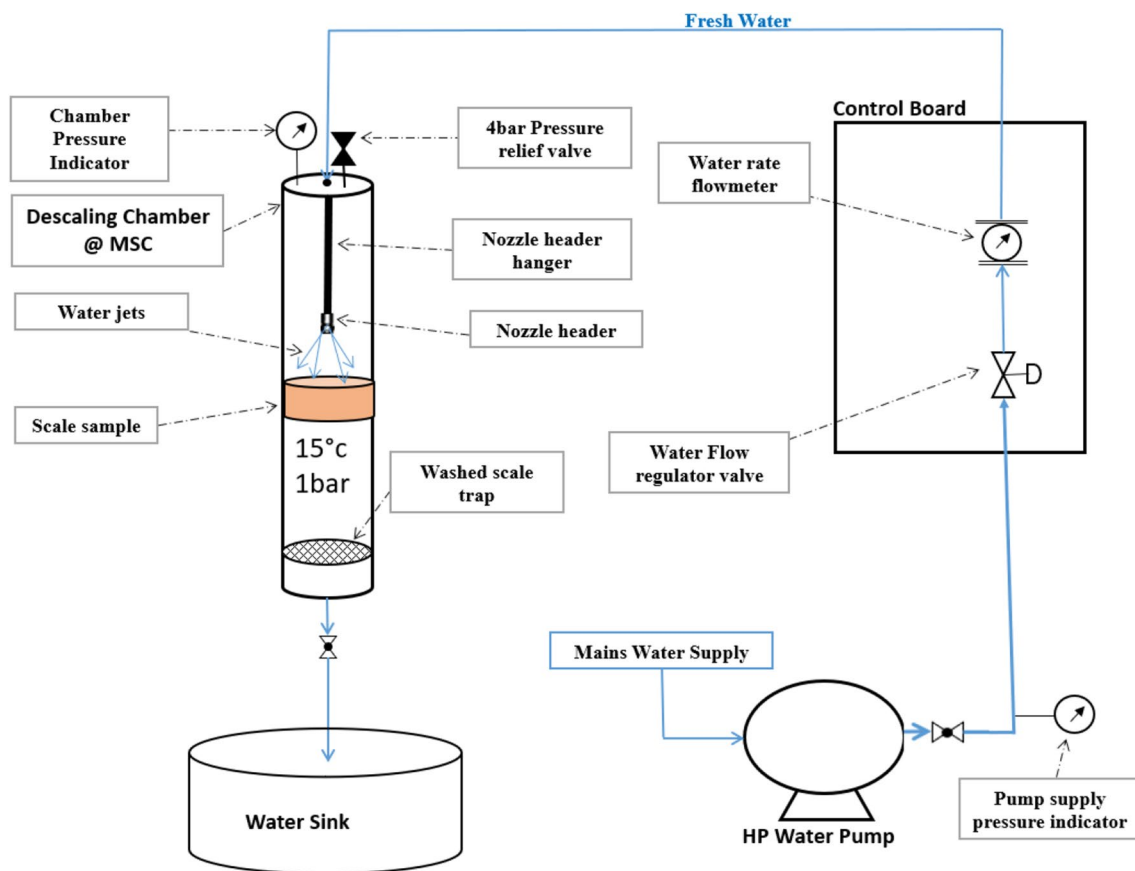


Fig. 3 Process diagram of descaling experiment at ambient chamber condition

positive correlation with the injection (jetting) pressure, but a negative correlation with the number of nozzles. Within the parameter space covered in this study, it is noteworthy that all the nozzle counts are characterized by a linear relationship between mass flux and jetting pressure. These results can readily be explained if one considers that the total flow area increases with the number of nozzles (or atomizers). Therefore, for the same mass flow rate, an increase in flow area causes a reduction in the mass flux. This explains the negative correlation between mass flux and nozzle count in Fig. 5.

As part of several quality-control measures implemented in these experiments, scale samples were tested for how closely they represented typical oil field paraffin scales. Figure 6 compares the cooling curve of the fabricated samples used in these experiments against published cooling curves of known paraffin waxes. Ignoring differences in samples, laboratory procedure and measurement uncertainties associated with the various experiments, the cooling behaviours of the samples and the reference paraffin waxes are considered reasonably comparable.

To compare the performances of the various experimental runs, we introduce the quantity, descaling efficiency (ϵ), as

a key performance indicator (KPI). This quantity is defined as follows.

$$\epsilon = \left(\frac{m_1 - m_2}{m_1} \right) \times 100\%, \quad (1)$$

where m_1 and m_2 are the masses of scale sample before and after descaling, respectively (g).

As presented in Tables 2 and 3, we recognize that the mass of scale samples varied between experiments. If these differences are not normalized, the interpretation of the experimental results will be biased. Therefore, the use of Eq. 1 to define a common KPI to discriminate all the descaling experiments precludes reaching potentially misleading conclusions when carrying out any comparative evaluation of the various runs.

Figure 7 displays descaling efficiency as a function of spray stand-off for different nozzle counts at a given jetting pressure (10 MPa) under ambient chamber conditions. In this context, spray stand-off is the direct distance between the nozzle surface and the surface of the target scale sample (Fig. 8). From these results, it is evident that descaling efficiency decreases with spray stand-off. However, in the range

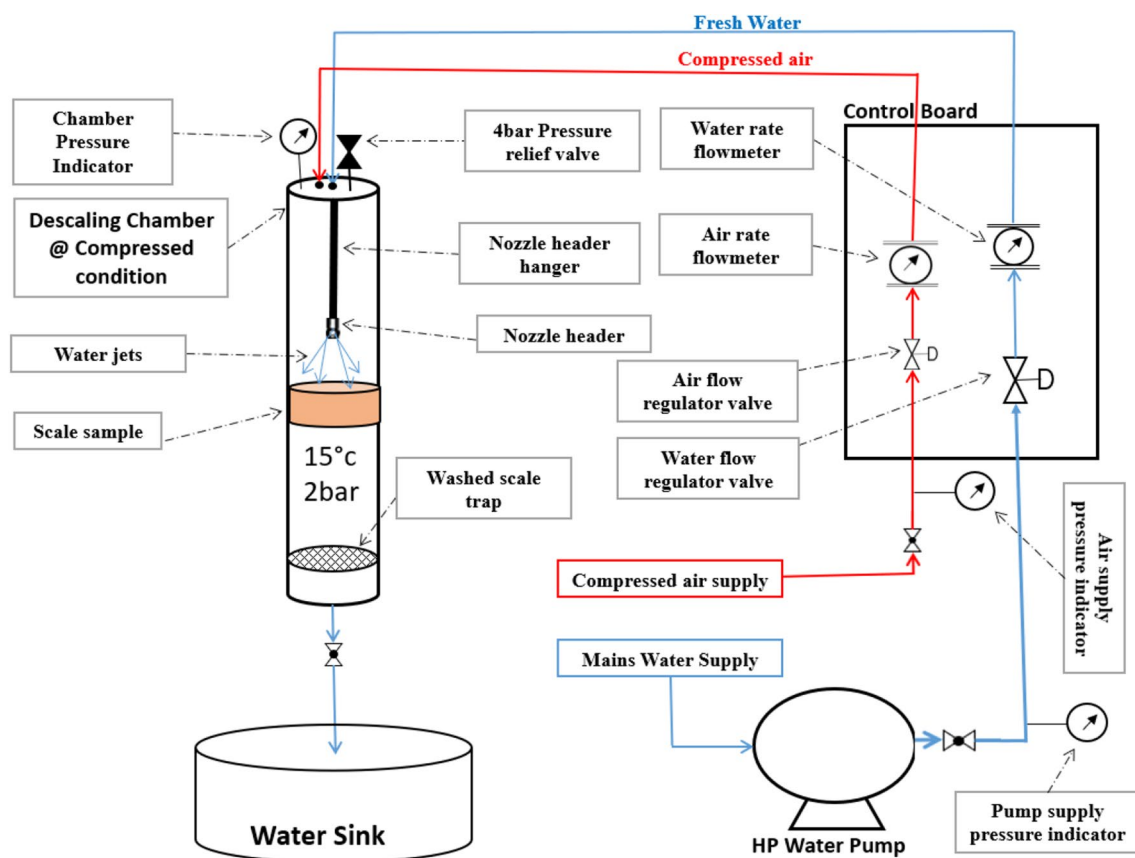


Fig. 4 Process diagram of descaling experiment at compressed chamber condition

Table 1 Results of rig calibration

| Number of nozzles | Mass flux ($\text{g}/\text{cm}^2 \cdot \text{s}$) | Injection pressure (MPa) | | |
|-------------------|-----------------------------------------------------|--------------------------|------------|---------------|
| | | Rig | Pump gauge | Control board |
| 5 | 1.1 | 4.8 | 10.0 | 5.8 |
| | 1.2 | 6.0 | 12.0 | 7.5 |
| | 1.8 | 10.0 | 19.0 | 15.0 |
| 4 | 1.5 | 4.8 | 9.0 | 6.0 |
| | 1.6 | 6.0 | 10.0 | 7.5 |
| | 2.2 | 10.0 | 16.5 | 13.5 |
| 3 | 2.1 | 4.8 | 4.0 | 5.0 |
| | 2.2 | 6.0 | 5.5 | 7.0 |
| | 2.6 | 10.0 | 14.0 | 12.0 |

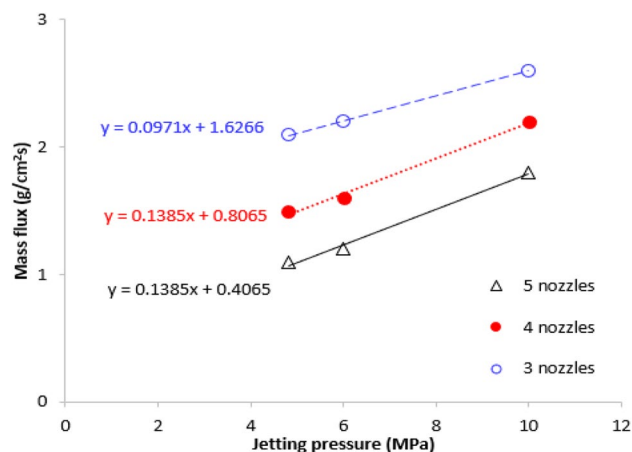


Fig. 5 Mass flux as a function of jetting pressure for the different nozzle counts examined

of spray stand-off investigated, the dependency of descaling efficiency on spray stand-off is consistently nonlinear for all the nozzle counts. Although space constraints preclude providing graphical illustrations of the results for the other jetting pressures and the case of compressed chamber conditions, similar trends such as those in Fig. 7 were recorded.

The foregoing observation of improvement in descaling efficiency with reducing spray stand-off and decreasing

nozzle count is not surprising. These trends can readily be explained by the tendency of the spray particles to exert higher impact forces on the scales at shorter stand-off distances. Similarly, lower nozzle count promotes higher mass flux (Fig. 5) which, in turn, increases the force impinging a

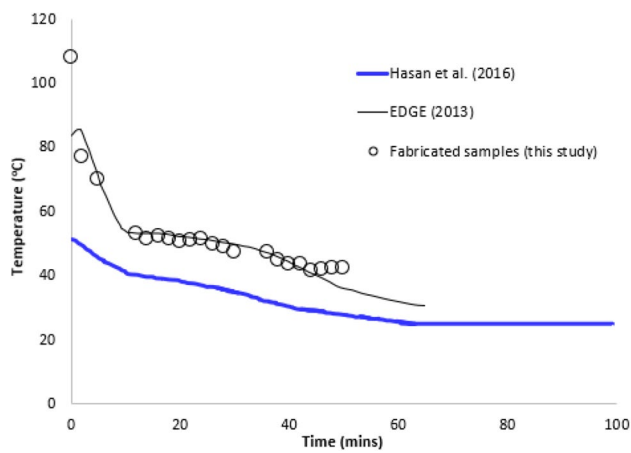


Fig. 6 Comparison of cooling curves of the scale samples against those of known paraffin waxes

target scale. It should be noted that the effects of the impact force on the target scale may take varied forms. Among other mechanisms, these distortion forms include erosion, breakage, piercing and cracking of the scale sample. The dominant forms for the individual experimental runs are indicated in Tables 2 and 3 for the ambient and compressed chamber conditions, respectively.

The veracity of the preceding explanation is supported by conducting a close inspection of the shape of a specific scale before and after descaling. For the 5-nozzle experiments, Figs. 16 and 17 provide pictures of various scale samples before and after descaling with jet water under ambient and compressed chamber conditions, respectively. Regardless of the experimental condition, it can be deduced that the original shape of the scales became more distorted as the spray stand-off reduced. This observation appears to be most pronounced at a jetting pressure of 10 MPa. This clearly shows that a shorter spray distance increases the impact force (erosional effects) which, in turn, induces greater and deeper

Table 2 Experimental runs and results of descaling under ambient chamber condition (all runs had a descaling time of 3 min during which targeted jetting was performed continuously)

| Run | No. of nozzles | Mass flow rate (g/s) | Mass jetted for descaling (kg) | Jetting pressure (MPa) | Nozzles config. | Stand-off (mm) | Scale ID | Scale mass before (g) | Scale mass after (g) | Descaling efficiency (%) | Remark |
|-----|----------------|----------------------|--------------------------------|------------------------|-----------------|----------------|----------|-----------------------|----------------------|--------------------------|--------|
| 1 | 5 | 434.0 | 78.1 | 4.8 | Pentagon | 25 | 17SH | 573.1 | 571.4 | 0.30 | Eroded |
| 2 | | | | | | 50 | 25SH | 520.9 | 520.0 | 0.17 | Eroded |
| 3 | | | | | | 75 | 44SH | 560.6 | 560.4 | 0.04 | Eroded |
| 4 | | 462.0 | 83.2 | 6 | Pentagon | 25 | 5SH | 574.9 | 572.0 | 0.50 | Eroded |
| 5 | | | | | | 50 | 73SH | 594.7 | 593.2 | 0.25 | Eroded |
| 6 | | | | | | 75 | 40SH | 569.3 | 568.9 | 0.07 | Eroded |
| 7 | 5 | 765.0 | 137.7 | 10 | Pentagon | 25 | 11SH | 568.9 | 510.6 | 10.25 | Broken |
| 8 | | | | | | 50 | 65SH | 533.7 | 523.9 | 1.84 | Eroded |
| 9 | | | | | | 75 | 42SH | 573.0 | 572.4 | 0.10 | Eroded |
| 10 | | 377.0 | 67.9 | 4.8 | Rectangle | 25 | 38SH | 542.7 | 536.5 | 1.14 | Hole |
| 11 | | | | | | 50 | 3SH | 544.8 | 542.2 | 0.48 | Eroded |
| 12 | | | | | | 75 | 58SH | 541.1 | 540.7 | 0.07 | Eroded |
| 13 | 5 | 411.0 | 74.0 | 6 | Rectangle | 25 | 8SH | 532.1 | 522.1 | 1.88 | Hole |
| 14 | | | | | | 50 | 59SH | 561.9 | 557.4 | 0.80 | Eroded |
| 15 | | | | | | 75 | 47SH | 575.2 | 574.6 | 0.10 | Eroded |
| 16 | | 608.0 | 109.4 | 10 | Rectangle | 25 | 10SH | 523.6 | 447.0 | 14.63 | Broken |
| 17 | | | | | | 50 | 70SH | 551.9 | 530.1 | 3.95 | Hole |
| 18 | | | | | | 75 | 49SH | 550.9 | 549.9 | 0.18 | Eroded |
| 19 | 3 | 313.0 | 56.3 | 4.8 | Triangle | 25 | 4SH | 580.9 | 538.1 | 7.37 | Hole |
| 20 | | | | | | 50 | 34SH | 551.1 | 541.4 | 1.76 | Hole |
| 21 | | | | | | 75 | 45SH | 569.4 | 568.3 | 0.19 | Eroded |
| 22 | | 306.0 | 55.1 | 6 | Triangle | 25 | 15SH | 659.7 | 566.0 | 14.20 | Broken |
| 23 | | | | | | 50 | 29SH | 557.7 | 542.5 | 2.73 | Hole |
| 24 | | | | | | 75 | 52SH | 580.9 | 579.5 | 0.24 | Eroded |
| 25 | 3 | 353.0 | 63.5 | 10 | Triangle | 25 | 21SH | 517.7 | 263.9 | 49.02 | Broken |
| 26 | | | | | | 50 | 67SH | 519.0 | 489.0 | 5.78 | Hole |
| 27 | | | | | | 75 | 51SH | 580.5 | 578.7 | 0.31 | Eroded |

destruction of the scale. A similar trend of increasing defects and distortion of scale sample with reducing spray stand-off is evident in the various 4 and 3-nozzle experiments under both ambient and compressed chamber conditions (Figs. 18, 19, 20, 21).

For a given number of nozzles and stand-off distance, the scale removal efficiency was found to increase as the water injection pressure increased (Fig. 9). For the range of jetting pressures investigated, the relationship between descaling efficiency and jetting pressure can be approximated by an exponential function. This positive correlation between descaling efficiency and jetting pressure is attributed to increased impact force occasioned by higher mass flux generated at high injection pressures (Fig. 5). In agreement with the other observations, there is a general trend of improved descaling efficiency with reduction in the number of nozzles (Fig. 9).

A close examination of Figs. 16, 17, 18, 19, 20 and 21 would provide further insights into the effects of jetting pressure on the efficiency of scale removal by a water jet. From these figures, one could deduce a general trend. The trend is such that, regardless of the spray stand-off and nozzle count, defects on the scale samples were more pronounced as the jetting pressure increased. Clearly, these results and the others underscore the importance of the impact of the spray jet in achieving effective scale removal. It is instructive to emphasize that the impact of the spray jet is controlled by (1) spray stand-off, (2) number of nozzles, and (3) jetting pressure. Although we recognize the importance of the spray angle to the descaling efficiency, the evaluation of this factor is outside the scope of this study.

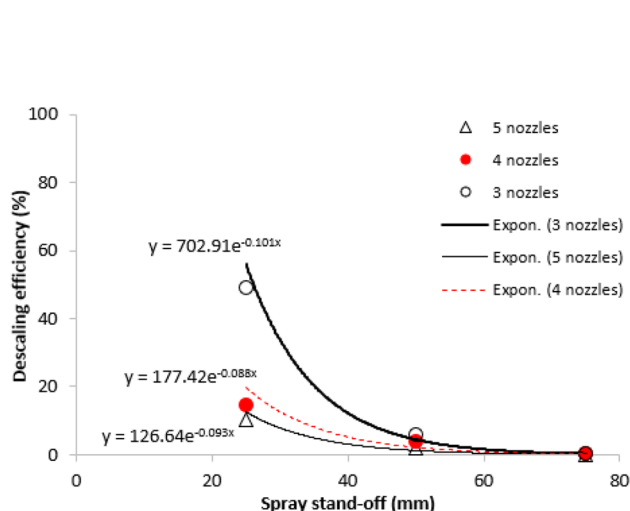


Fig. 7 Effects of nozzle count and spray stand-off on descaling efficiency (10 MPa jetting pressure, ambient chamber). Validity of the empirical models is limited to the stand-off range 25–75 mm

Although it is common knowledge that heating (or rise in temperature) causes melting, which explains why heating, along with chemical treatment, is one of the major ways by which the Oil and Gas Industry handles scale problems in pipelines, heating of pipelines covering huge land masses and lengthy distances is expensive. In line with that, another objective of this research, besides alleviating the use of chemical inhibitors for oilfield descaling, is to encourage the replacement of chemical inhibitors and pipe-heating with low-cost, clean water jets at room temperatures. Consequently, the effect of in situ temperature and the temperature of the jet fluid on the scale removal rate were also not considered within the scope of this study.

Figure 10 compares the effects of chamber conditions on the efficiency of scale removal for the specific range of spray distance considered in this study. For all practical purposes, the chamber condition does not appear to have significant influence on descaling efficiency for the set of experiments conducted. It is worthwhile to mention that the interpretation of Fig. 10 should be put in the proper context. Specifically, it should be noted that the so-called ambient and compressed chamber environments in this study are characterized by in situ pressures of 1 bar and 2 bar, respectively. In principle, this pressure difference is not considered large enough to cause a major impact on descaling efficiency. This notwithstanding, a careful inspection of Figs. 16, 17, 18, 19, 20 and 21, suggests that, on a general note, the degree of sample deformation appears to be more pronounced under compressed chamber conditions than the corresponding ambient environment.

Therefore, considering that Fig. 10 does not provide sufficient quantitative discrimination between ambient and compressed descaling conditions, we recommend, as a potential

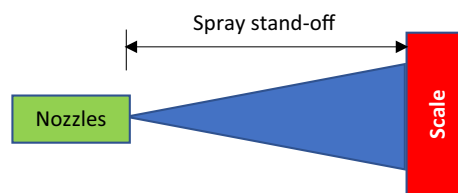


Fig. 8 Schematic of scale removal by jetting, illustrating a spray stand-off

improvement area in future studies, that the use of water jets for descaling should consider environments of much higher pressures to simulate typical field conditions. Such test environments, preferably above 20 bar and 40 °C would provide better insights into the dynamics and efficacy of water jets for scale removal in production tubings and similar facilities.

As part of this study, we paid attention to the nature of deformation on each sample after undergoing the process of

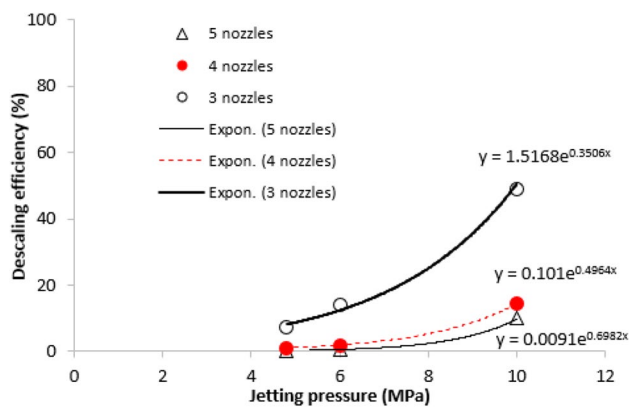


Fig. 9 Effects of nozzle count and jetting pressure on descaling efficiency (25 mm spray stand-off, ambient chamber). Validity of the empirical models is limited to jetting pressures of 4.8–10.0 MPa

scale removal by water jetting. Although multiple deformation types were seen on some samples, we report the dominant type of defect induced by the spray jet on each sample. As indicated in Tables 2 and 3, the main deformation types seen are breakage, erosion, hole, pierce and crack.

Figure 11 illustrates the distribution of deformation types as a function of chamber conditions. The plot suggests that some 60% and 52% of the sample populations were deformed by erosion under ambient (1 bar) and pressurized (2 bar) chamber conditions, respectively. Other important deformations are the creating of holes and breakage of some samples. In the 54 experimental runs performed, piercing and cracking defects were limited to few samples in a compressed environment.

Figure 12 shows the statistics of dominant deformation types as a function of jetting pressure for experiments performed under ambient condition. Regardless of the jetting pressure, erosion was found to be the primary cause of deformation. Specifically, 44% of the samples were eroded at 10 MPa, while 67% of the population were eroded when exposed to 4.8 MPa and 6 MPa spray pressures in an ambient environment. While some samples got broken at 6 MPa and 10 MPa, none of the samples experienced breakage at 4.8 MPa.

The distribution of deformation types as a function of spray distance for experiments executed at an ambient condition is displayed in Fig. 13. It is worthy of note that all the samples were eroded when exposed to a 75 mm spray distance. Owing to the inverse relationship between impact force and spray distance, it is not surprising that erosion was found to be the dominant mechanism of deformation at such a relatively high spray distance. Conversely, the increased impact force associated with a shorter spray distance explains why breakage and hole defects dominated the case of 25 mm spray stand-off.

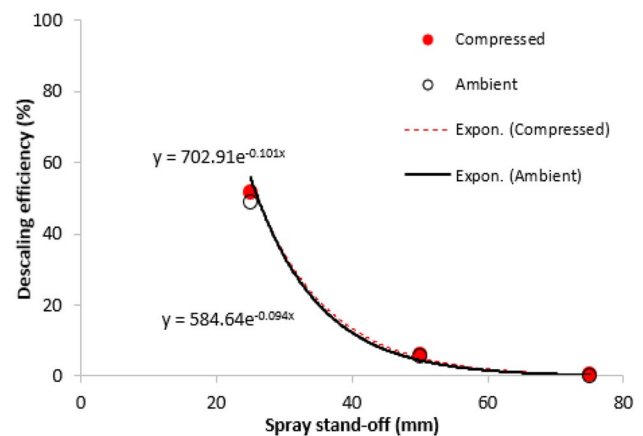


Fig. 10 Effects of spray stand-off and chamber condition on descaling efficiency (3 nozzles, 10 MPa jetting pressure). Validity of the empirical models is limited to the stand-off range 25–75 mm

Figure 14 presents the statistics of deformation types as a function of injection pressure under compressed chamber conditions. Consistent with the observations in the ambient environment (Fig. 12), erosion remained the main mechanism by which most of the samples were descaled for the three cases of injection pressure investigated. However, while all the five deformation mechanisms were noticed in the 10 MPa case, this is not quite the same for the other injection pressure cases. For example, at 4.8 MPa, breakage and cracking were not reported. Similarly, piercing and cracking were generally absent in all cases of 6 MPa injection in the compressed environment.

In Fig. 15, the statistics of deformation types are displayed for different spray distances for experiments conducted under compressed chamber conditions. In agreement with the results under ambient conditions (Fig. 13), erosion remained the primary mechanism of descaling the samples. But in the case of 25 mm stand-off, breakage was pronounced. In terms of the number of damage mechanisms at play, the cases of 25 mm and 50 mm spray stand-off experienced four each, while 75 mm had only one. This suggests that the number of active deformation mechanisms increases as the stand-off distance reduces. As a result, we speculate that the predictability of the number and type of active deformation would become more difficult and uncertain as the spray stand-off decreases as suggested by the distributions depicted in Figs. 13 and 15.

Conclusion

Employing multiple flat-fan nozzles at an orientation of 25°, a set of laboratory experiments was designed and executed to understand the technical feasibility of high-pressure water jets for scale removal in both ambient and mild-pressure

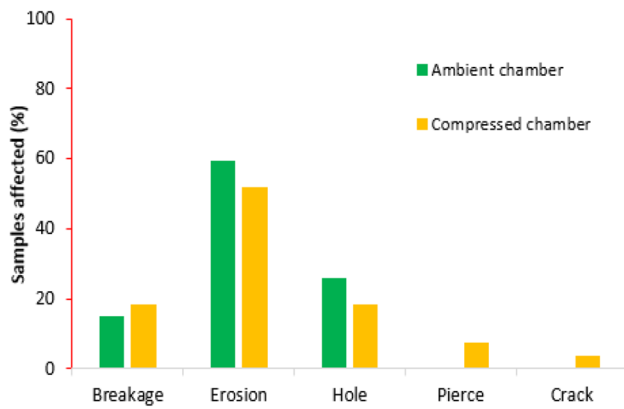


Fig. 11 Dominant deformation types inflicted on scale samples at ambient and compressed chamber conditions

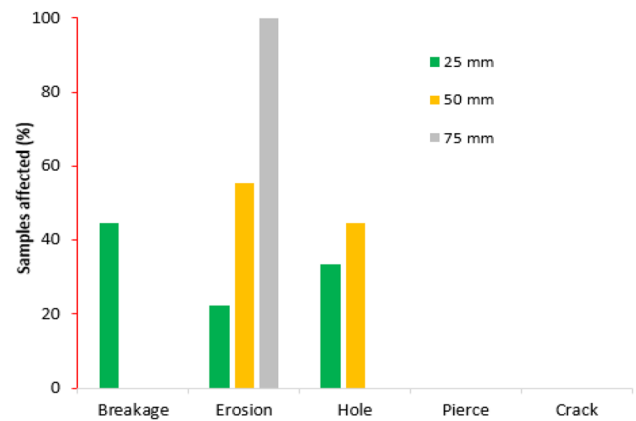


Fig. 13 Distribution of deformation types as a function of spray stand-off (ambient chamber)

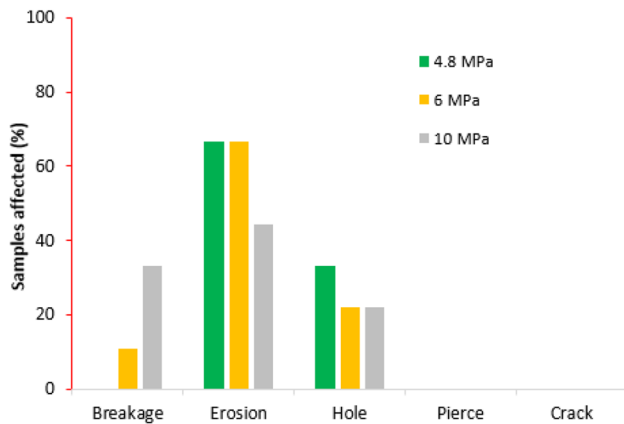


Fig. 12 Distribution of deformation types as a function of jetting pressure (ambient chamber)

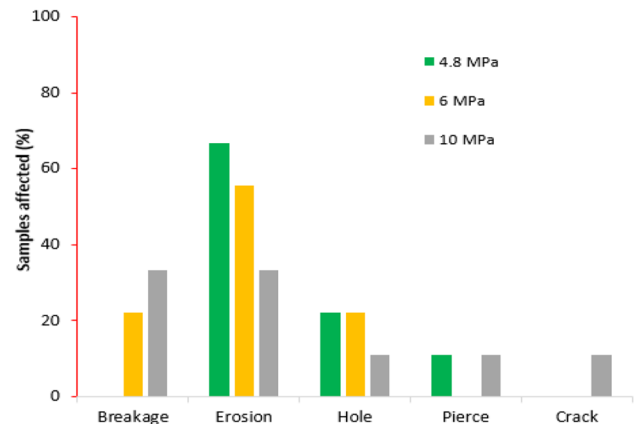


Fig. 14 Distribution of deformation types as a function of jetting pressure (compressed chamber)

(2 bar) environments. With these controlled experiments, the impacts of four key factors were investigated vis-à-vis (1) number of nozzles; (2) spray injection pressure; (3) stand-off distance between the spray nozzle and target scale; and (4) condition of the production tubing, both ambient and pressurized.

The results of these experiments showed that the use of high-pressure water jets as a cleaner method of descaling is technically feasible. For the range of parameters examined, it was observed that erosion was the dominant mechanism of scale removal by this water-jet technique at both ambient and compressed chamber conditions. To a large extent, contributions of the scale-deformation mechanisms of piercing and cracking were found to be limited in this study.

Within the parameter space explored, the descaling efficiency of a water jet exhibited an exponential increase with the jetting pressure, but an exponential decrease with spray stand-off, defined as the distance between the spray nozzles and target scales. Additionally, under ambient and

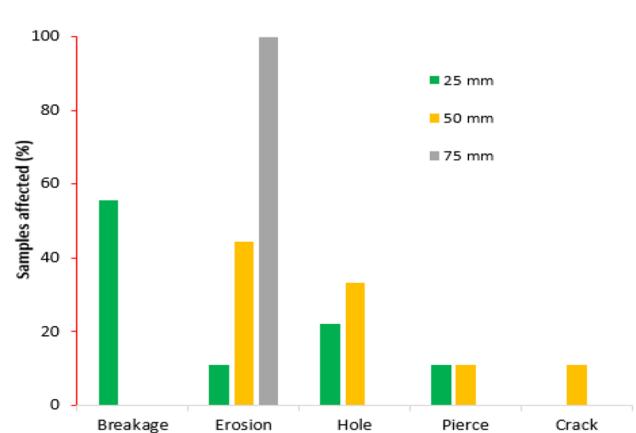


Fig. 15 Distribution of deformation types as a function of spray stand-off (compressed chamber)

compressed environments, descaling efficiency showed a negative correlation with the number of active nozzles of the water jet. However, for the 1 bar and 2 bar conditions

investigated, the prevailing pressure condition of the operating environment did not appear to have significant influence on the efficiency of scale removal by a water jet. Based on this outcome, it can be concluded that the combination of practicable minimum stand-off distance, minimum nozzle count and maximum jetting pressure offers the best opportunity to maximize the performance of a water jet at remediating paraffin scale problem in a production tubing and other scale-prone facilities in practice.

As an improvement on this study, the effects of varying the nozzle orientation of a water jet on descaling efficiency should be investigated. Furthermore, as a better check of the representativeness of fabricated scale samples versus oil field soft scales, samples representativeness tests should include hardness and structural tests. Furthermore, to reduce discrepancies in the properties of the soft scale samples, they should be produced in a single batch. Multi-batch production creates variations in hardness and dryness of the scale samples.

Finally, future studies on the use of water jets for descaling should be carried out under more realistic conditions like the removal of actual paraffin scales at in situ field conditions. Such studies would provide better insights into the dynamics and efficacy of water jets for scale removal in field production tubings and similar facilities.

Acknowledgements I.J. John is grateful to the Nigerian government, through the Petroleum Technology Development Fund (PTDF), for sponsoring his MSc program at the University of Salford, Manchester. Financial support from the PTDF scholarship was instrumental to the success of this research.

Funding The authors received no specific funding for this work.

Open Access This article is licensed under a Creative Commons Attribution 4.0 International License, which permits use, sharing, adaptation, distribution and reproduction in any medium or format, as long as you give appropriate credit to the original author(s) and the source, provide a link to the Creative Commons licence, and indicate if changes were made. The images or other third party material in this article are included in the article's Creative Commons licence, unless indicated otherwise in a credit line to the material. If material is not included in the article's Creative Commons licence and your intended use is not permitted by statutory regulation or exceeds the permitted use, you will need to obtain permission directly from the copyright holder. To view a copy of this licence, visit <http://creativecommons.org/licenses/by/4.0/>.

Appendix A: Procedure for descaling experiment at ambient conditions

- i. Twenty-seven independent experimental runs were designed, such that each run was assigned different combinations of design factors (variables), i.e. the number of nozzles, stand-off distance, injection pressure and nozzle configuration. For robustness, the technique of experimental design (ED) was employed.
- ii. A scale sample was allotted per experimental run, with a unique scale identifier (ID) recorded against each run.
- iii. Scale samples were weighed and their masses before spraying recorded against the run number. This updates the experimental design to the bold columns (Column 2–Column 9) of Table 2.
- iv. The image of each scale was taken and recorded before the spraying.
- v. For the first experiment, run 1 (row 2 in Table 2), 5 atomizers were fitted on the nozzle header to obtain a pentagon configuration.
- vi. The corresponding scale sample (17-SH in this case) was placed on the holder.
- vii. The corresponding stand-off distance (25 mm in this case) was obtained by placing only the 50 mm stand-off distance adjustment ring between the scale holder and the bottom plate of the descaling chamber.
- viii. The washed scale debris trap was placed between the water outlet and the stand-off distance adjustment ring.
- ix. The acrylic tube was gently placed on the bottom plate such that the scale sample, holder and washed scale traps were inserted into the tube.
- x. The chamber header assembly was gently fitted on the acrylic tube.
- xi. The descaling chamber was adjusted and secured properly for structural integrity and to ensure that a water-tight column was created when the water outlet valve was closed.
- xii. The HP pump was switched on and freshwater sprayed on the scale sample at the pressure corresponding to this run (4.8 MPa) for 3 min.
- xiii. The scale sample was removed from the chamber and an image of the scale was taken and recorded.
- xiv. The scale sample was subjected to 12 h of indoor drying. Afterwards, it was weighed, and the mass recorded against the experimental run number and scale ID.
- xv. The washed scale trap/sieve was cleaned of the debris removed from the scale sample.
- xvi. Steps iii to xv were repeated for the remaining 26 experimental runs (i.e. runs 2–27, Table 2) using the specified parameters and corresponding scale in the experimental design for each run.
- xvii. The mass of scale removed was obtained as the difference between its mass before and after spraying, reflecting the impacts (erosion and/or creation of a hole) of spraying on the scale.

Table 3 Experimental runs and results of descaling under compressed chamber condition (all runs had a descaling time of 3 min during which targeted jetting was performed continuously)

| Run | No. of nozzles | Mass flow rate (g/s) | Mass jetted for descaling (kg) | Jetting pressure (MPa) | Nozzles config. | Stand-off (mm) | Scale ID | Scale mass before (g) | Scale mass after (g) | Descaling efficiency (%) | Remark |
|-----|----------------|----------------------|--------------------------------|------------------------|------------------|----------------|--------------|-----------------------|----------------------|--------------------------|---------|
| 1 | 5 | 434.0 | 78.1 | 4.8 | Pentagon | 25 | 21SHA | 555.9 | 553.1 | 0.50 | Eroded |
| 2 | | | | | | 50 | 4SHA | 571.4 | 570.1 | 0.23 | Eroded |
| 3 | | | | | | 75 | 69SHA | 562.7 | 562.3 | 0.07 | Eroded |
| 4 | | 462.0 | 83.2 | 6 | Pentagon | 25 | 55SHA | 519.3 | 514.0 | 1.02 | Hole |
| 5 | | | | | | 50 | 65SHA | 573.9 | 572.0 | 0.33 | Eroded |
| 6 | | | | | | 75 | 5-SHA | 544.7 | 544.1 | 0.11 | Eroded |
| 7 | | 765.0 | 137.7 | 10 | Pentagon | 25 | 38SHA | 529.1 | 460.7 | 12.93 | Broken |
| 8 | | | | | | 50 | 27SHA | 528.3 | 516.1 | 2.31 | Hole |
| 9 | | | | | | 75 | 44SHA | 597.3 | 596.4 | 0.15 | Eroded |
| 10 | 4 | 377.0 | 67.9 | 4.8 | Rectangle | 25 | 11SHA | 571.3 | 562.0 | 1.63 | Hole |
| 11 | | | | | | 50 | 25SHA | 537.5 | 534.4 | 0.58 | Eroded |
| 12 | | | | | | 75 | 46SHA | 519.8 | 519.1 | 0.13 | Eroded |
| 13 | | 411.0 | 74.0 | 6 | Rectangle | 25 | 7SHA | 510.0 | 495.1 | 2.92 | Broken |
| 14 | | | | | | 50 | 67SHA | 517.3 | 511.5 | 1.12 | Eroded |
| 15 | | | | | | 75 | 52SHA | 567.2 | 566.2 | 0.18 | Eroded |
| 16 | | 608.0 | 109.4 | 10 | Rectangle | 25 | 12SHA | 585.5 | 435.1 | 25.69 | Broken |
| 17 | | | | | | 50 | 28SHA | 576.1 | 549.2 | 4.67 | Cracked |
| 18 | | | | | | 75 | 48SHA | 553.5 | 551.7 | 0.33 | Eroded |
| 19 | 3 | 313.0 | 56.3 | 4.8 | Triangle | 25 | 29SHA | 571.7 | 482.6 | 15.59 | Pierced |
| 20 | | | | | | 50 | 34SHA | 565.9 | 553.2 | 2.24 | Hole |
| 21 | | | | | | 75 | 51SHA | 554.3 | 552.9 | 0.25 | Eroded |
| 22 | | 306.0 | 55.1 | 6 | Triangle | 25 | 13SHA | 531.6 | 323.4 | 39.16 | Broken |
| 23 | | | | | | 50 | 76SHA | 529.7 | 508.1 | 4.08 | Hole |
| 24 | | | | | | 75 | 81SHA | 548.7 | 546.9 | 0.33 | Eroded |
| 25 | | 353.0 | 63.5 | 10 | Triangle | 25 | 24SHA | 564.8 | 273.3 | 51.61 | Broken |
| 26 | | | | | | 50 | 36SHA | 583.7 | 548.9 | 5.96 | Pierced |
| 27 | | | | | | 75 | 79SHA | 570.0 | 567.4 | 0.46 | Eroded |

xviii. Where the scale was either broken or shattered, the mass of the largest chunk was taken as its mass after the experiment in step xvii.

xix. The results for all the 27 runs performed under ambient conditions are tabulated in Table 2.

Appendix B: Procedure for descaling experiment at compressed conditions

- Steps i–x of “Appendix A” were repeated with 27 new (and different) scales per the ED. The experimental runs are outlined in Table 3 (bold columns 2–9).
- A compressed air circulation system was connected to the rig as shown in Fig. 3 and the descaling chamber was coupled to be airtight and structurally stable.

- The water outlet valve in the bottom plate was closed and compressed air injected into the chamber until the chamber pressure gauge indicated 2 bar (~202 kPa).
- The HP pump was then switched on and freshwater sprayed on the scale sample at the pressure (4.8 MPa) corresponding to this run for 3 min.
- The chamber pressure was kept at 2 bar with the use of a column of water to seal off the water outlet; such that a closed, compressive environment was maintained around the scale sample even as the water outlet valve was opened and water circulated during the experimental run time.
- At the end of the 3 min run time, the air supply was cut off and steps xiii–xviii of “Appendix A” repeated on this scale sample and in line with the scheme in Table 3 (the design for this experiment).

The results for all the 27 runs performed under compressed conditions are tabulated in Table 3.

Appendix C: Some qualitative results

See Figs. 16, 17, 18, 19, 20 and 21.

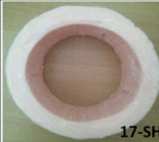

















| 5 NOZZLES Ambient Chamber | | BEFORE DESCALING | | AFTER DESCALING | | BEFORE DESCALING | | AFTER DESCALING | | BEFORE DESCALING | | AFTER DESCALING | |
|---------------------------------|--------|-----------------------------------------------------------------------------------|-----------------------------------------------------------------------------------|-----------------------------------------------------------------------------------|------------------------------------------------------------------------------------|-------------------------------------------------------------------------------------|-------------------------------------------------------------------------------------|--------------------|--|---------------------|--|--------------------|--|
| Injection Pressure | 4.8MPa |  |  |  |  |  |  | | | | | | |
| | 6MPa |  |  |  |  |  |  | | | | | | |
| | 10MPa |  |  |  |  |  |  | | | | | | |
| | | 25mm | | 50mm | | 75mm | | | | | | | |
| | | Stand-off distance | | | | | | | | | | | |

Fig. 16 Scale samples before and after descaling experiments with 5 nozzles (ambient chamber)

| 5 NOZZLES Compressed Chamber | | BEFORE DESCALING | AFTER DESCALING | BEFORE DESCALING | AFTER DESCALING | BEFORE DESCALING | AFTER DESCALING |
|------------------------------------|--------|-------------------------------------------------------------------------------------|-------------------------------------------------------------------------------------|-------------------------------------------------------------------------------------|--------------------------------------------------------------------------------------|---------------------------------------------------------------------------------------|---------------------------------------------------------------------------------------|
| Injection Pressure | 4.8MPa |  |  |  |  |  |  |
| | 6MPa |  |  |  |  |  |  |
| | 10MPa |  |  |  |  |  |  |
| | | 25mm | | 50mm | | 75mm | |
| | | Stand-off distance | | | | | |

Fig. 17 Scale samples before and after descaling experiments with 5 nozzles (compressed chamber)

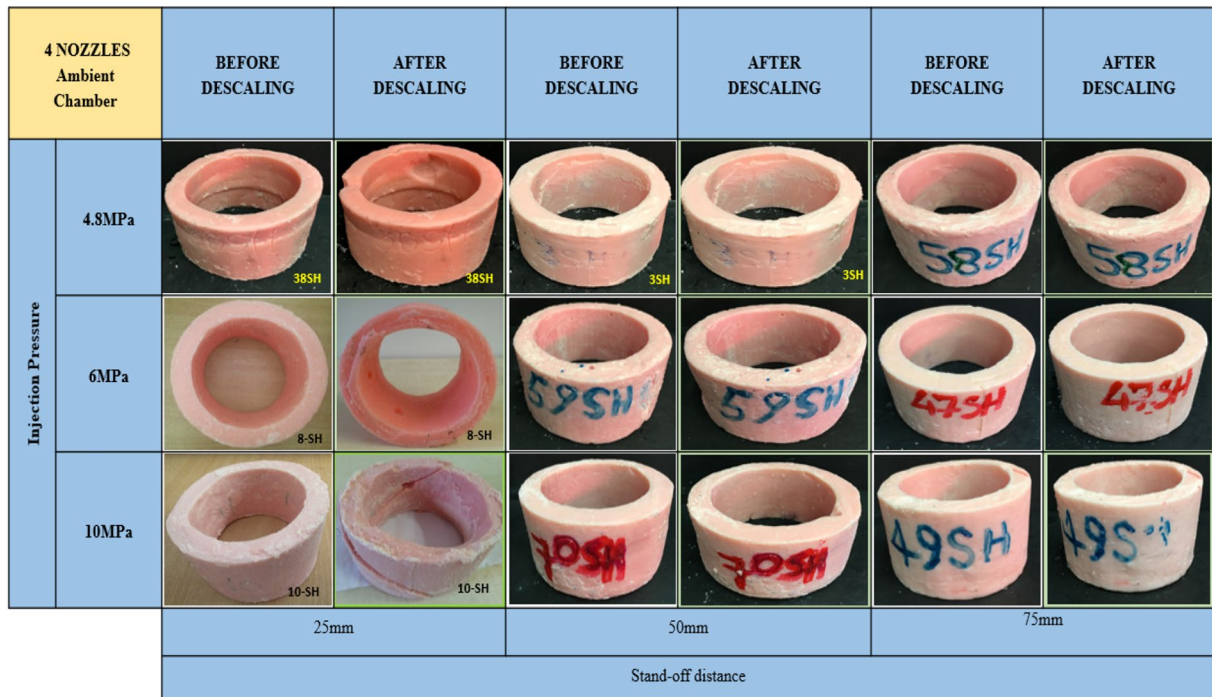


Fig. 18 Scale samples before and after descaling experiments with 4 nozzles (ambient chamber)

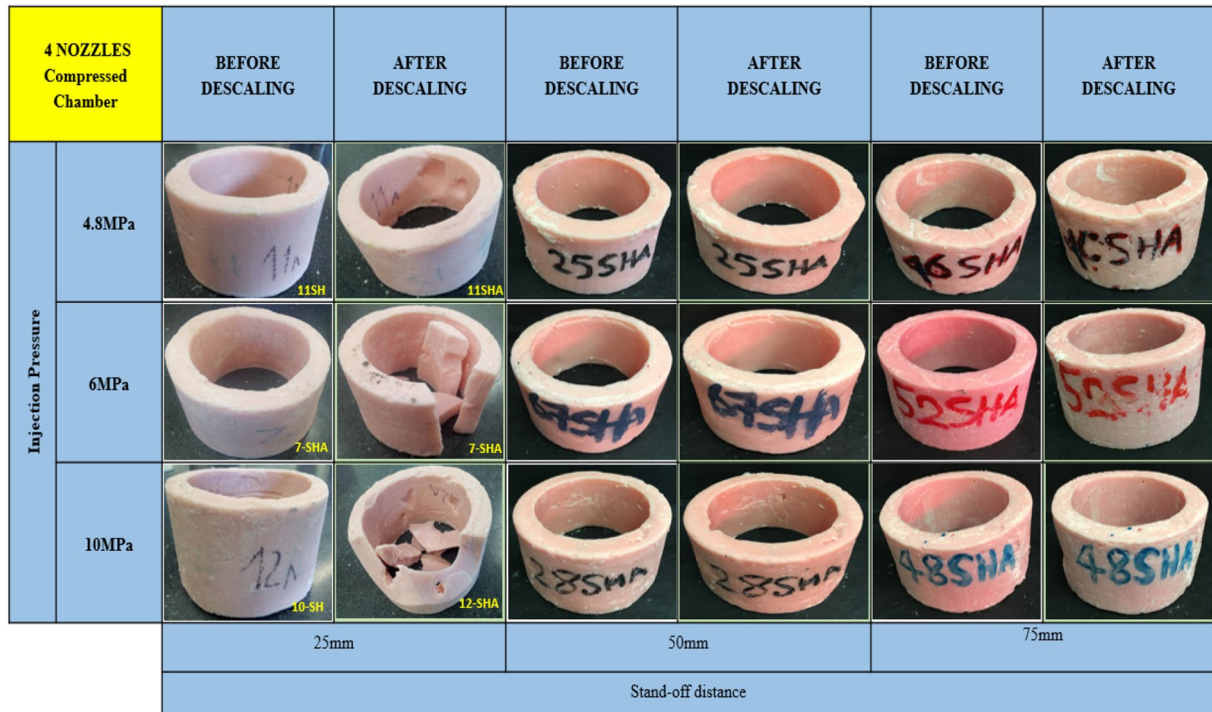


Fig. 19 Scale samples before and after descaling experiments with 4 nozzles (compressed chamber)

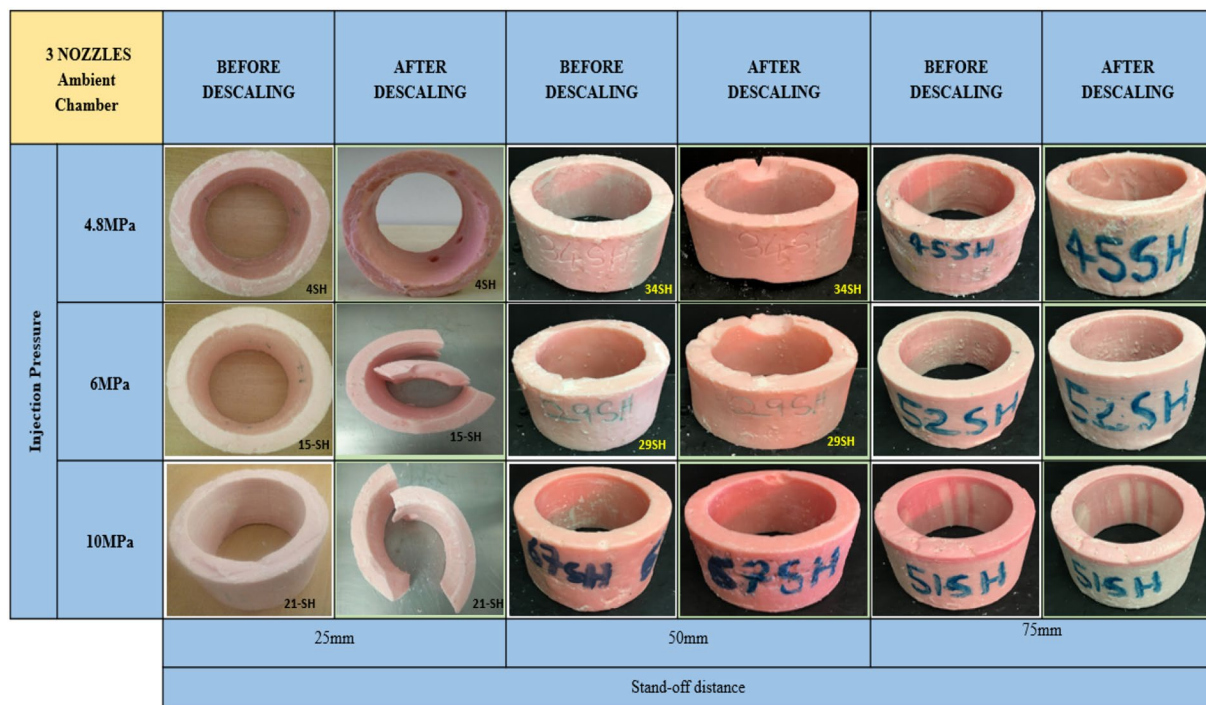


Fig. 20 Scale samples before and after descaling experiments with 3 nozzles (ambient chamber)



Fig. 21 Scale samples before and after descaling experiments with 3 nozzles (compressed chamber)

References

- Abbas AJ (2014) Descaling of petroleum production tubing utilising aerated high-pressure flat fan water sprays, Ph.D. thesis, The University of Salford, Manchester
- Abbas AJ, Nasr GG, Nourian A, Enyi GC (2015) Impact pressure distribution in flat fan nozzles for descaling oil wells. Paper ICLASS 2015, presented at 13th triennial international conference on liquid atomization and spray systems, 23–27 Aug., Tainan
- Akinyemi O, Udonne J, Oyedeko K (2018) Study of effects of blend of plant seed oils on wax deposition tendencies of Nigerian waxy crude oil. *J Pet Sci Eng* 161:551–558
- Amjad Z, Koutsoukos P (2010) Mineral Scales and Deposits. IWA Publishing, London, UK. <https://doi.org/10.1201/9781420071450-c1>
- Borden K (2014) Flow assurance: hydrates and paraffin management. *Oil Gas Facil* 3(1):29–33
- Braun G, Boles JL (2007) Characterization and removal of amorphous aluminosilicate scales. SPE paper 24068, presented at SPE Western Regional Meeting, 30 Mar.–1 Apr., Bakersfield
- Chi Y, Daraboina N, Sarica C (2016) Investigation of inhibitors efficacy in wax deposition mitigation using a laboratory scale flow loop. *AIChE J* 62:4131–4139
- Crabtree M, Johnson A, Eslinger D, Fletcher P, Miller M, Johnson A, King G (1999) Fighting scale—removal and prevention. *Oilfield Rev* 11:30–45
- EDGE (2013) 100% wax cooling curve and melting point. <http://edge.rut.edu/edge/P13411/public/Wax> Test Data. Accessed 21 May 2019
- Elmorsey SA (2013) Challenge and successful application for scale removal Gamsa oil field, Egypt: field study. SPE paper 164274, presented at SPE Middle East oil and gas show and conference, 10–13 Mar., Manama
- Fulford RS (1975) Oilwell paraffin prevention chemicals. SPE paper 5611, presented at Fall meeting of the SPE of AIME, 28 Sept.–1 Oct., Dallas
- Guimaraes Z, Almeida V, Duque LH, Costa G, Pinto JC, Chagas JV, Coutinho S, Franca AB, Gouveia M, Peixoto C, Alberto C (2008) Efficient offshore scale removal without a rig: planning, logistics and execution. SPE paper 113783, presented at the SPE/ICoTa coiled tubing and well intervention conference and exhibition, 1–2 Apr., The Woodlands
- Hamdy E, Abu Bakr M, Abd El-Hay A, Sisostri S, Anwar M El Farouk O (2014) Challenge and successful application for scale removal in oil field, Egypt: field study. IPTC paper 18139, presented at International petroleum technology conference, 10–12 Dec., Kuala Lumpur
- Hasan A, Hejase H, Abdelbaqi S, Assi A, Hamdan MO (2016) Comparative effectiveness of different phase change materials to improve cooling performance of heat sinks for electronic devices. *Appl Sci* 6(226):1–20
- Lawal KA (2011) Alternating injection of steam and CO₂ for thermal recovery of heavy oil, Ph.D. thesis, Imperial College London
- Lawal KA, Vesovic V, Boek ES (2011) Modeling permeability impairment in porous media due to asphaltene deposition under dynamic conditions. *Energy Fuels* 25(12):5647–5659
- Lawal KA, Crawshaw JP, Boek ES, Vesovic V (2012) Experimental investigation of asphaltene deposition in capillary flow. *Energy Fuels* 26(4):2145–2153
- Leporini M, Terenzi A, Marchetti B, Giacchetta G, Corvaro F (2019) Experiences in numerical simulation of wax deposition in oil and multiphase pipelines: theory versus reality. *J Pet Sci Eng* 174:997–1008
- Mansoori H, Mobedifard V, Kouhpeyma AM (2017) Study finds simulation flaws in multiphase environment. *Oil Gas J* 112(11):102–105
- Moghadasi J, Jamialahmadi M, Müller-Steinhagen H, Sharif A (2003a). “Scale formation in oil reservoir and production equipment during water injection (kinetics of CaSO₄ and CaCO₃ crystal growth and effect on formation damage). SPE paper 82233, presented at the SPE European Formation Damage Conference, 13–14 May, The Hague
- Moghadasi J, Jamialahmadi M, Müller-Steinhagen H, Sharif A, Ghalambor A, Izadpanah MR, Motaie E (2003b) Scale formation in Iranian oil reservoir and production equipment during water injection. SPE paper 80406, presented at the international symposium on oilfield scale, 29–30 Jan., Aberdeen
- Nejad AM, Karimi MS (2017) Investigation of the influence of scaling on corrosion behaviour of tubing in oil wells. *Int J Sci Technol Res* 6(5):109–113
- Peng Y, Guo Z (2017) On the sweet corrosion of oil and gas wells. *Int J Sci Eng Invest* 6(64):25–27
- Ragunathan T, Husin H, Wood CD (2020) Wax formation mechanisms wax chemical inhibitors and factors affecting chemical inhibition. *Appl Sci* 10(479):1–18
- Sutton GD (1976) Aqueous systems for paraffin removal. SPE paper 5704, presented at the SPE Symposium on Formation Damage Control, 29–30 Jan., Houston
- Theyab MA (2017) Study of fluid flow assurance in hydrocarbon production—investigation wax mechanisms, Ph.D. thesis, London South Bank University, London
- Vazirian MM, Charpentier T, Penna M, Neville A (2015) Surface inorganic scale formation in oil and gas industry: as adhesion and deposition processes. *J Pet Sci Eng* 137:22–32

Publisher's Note Springer Nature remains neutral with regard to jurisdictional claims in published maps and institutional affiliations.